April 1, 1999

Radar and satellite global equatorial F-region vertical drift model

L. Scherliess
Bela G. Fejer, *Utah State University*

JOURNAL OF GEOPHYSICAL RESEARCH, VOL. 104, NO. A4, PAGES 6829–6842, APRIL 1, 1999

Radar and satellite global equatorial F region vertical drift model

L. Scherliess and B. G. Fejer

Center for Atmospheric and Space Sciences, Utah State University, Logan

Abstract. We present the first global empirical model for the quiet time F region equatorial vertical drifts based on combined incoherent scatter radar observations at Jicamarca and Ion Drift Meter observations on board the Atmospheric Explorer E satellite. This analytical model, based on products of cubic-B splines and with nearly conservative electric fields, describes the diurnal and seasonal variations of the equatorial vertical drifts for a continuous range of all longitudes and solar flux values. Our results indicate that during solar minimum, the evening prereversal velocity enhancement exhibits only small longitudinal variations during equinox with amplitudes of about 15-20 m/s, is observed only in the American sector during December solstice with amplitudes of about 5-10 m/s, and is absent at all longitudes during June solstice. The solar minimum evening reversal times are fairly independent of longitude except during December solstice. During solar maximum, the evening upward vertical drifts and reversal times exhibit large longitudinal variations, particularly during the solstices. In this case, for a solar flux index of 180, the June solstice evening peak drifts maximize in the Pacific region with drift amplitudes of up to 35 m/s, whereas the December solstice velocities maximize in the American sector with comparable magnitudes. The equinoctial peak velocities vary between about 35 and 45 m/s. The morning reversal times and the daytime drifts exhibit only small variations with the phase of the solar cycle. The daytime drifts have largest amplitudes between about 0900 and 1100 LT with typical values of 25-30 m/s. We also show that our model results are in good agreement with other equatorial ground-based observations over India, Brazil, and Kwajalein.

1. Introduction

Ionospheric electric fields play important roles on the plasma distribution and dynamics of the equatorial and low-latitude thermosphere. At equatorial latitudes, ionospheric electric fields drive the equatorial electrojet and F region plasma motions and affect the thermospheric neutral winds, the development of the Appleton anomaly, the composition of the low-latitude ionosphere and protonosphere, and the generation of E and F region plasma instabilities [e.g., *Fejer*, 1997].

The quiet time low-latitude plasma drifts are driven by a complex interaction of E and F region electrodynamic processes [e.g., *Richmond*, 1995]. The relative efficiency of these dynamo mechanisms varies significantly with the time of day, from day to day, and also with season, solar cycle, and longitude. At equatorial latitudes, to first order, the F region electrodynamic plasma drifts are upward and westward during the day and downward and eastward at night. During magnetically disturbed conditions, magnetospheric and disturbance dynamo effects can dramatically affect the low-latitude drifts [e.g., *Fejer and Scherliess*, 1997; *Scherliess and Fejer*, 1997].

Incoherent scatter radar observations at Jicamarca have provided the major source of information about the equatorial F region vertical and zonal electrodynamic ($\mathbf{E}\times\mathbf{B}$) plasma drifts [*Fejer et al.*, 1979, 1989, 1991]. Ionosonde observations in the Peruvian, Brazilian, and Indian equatorial sectors have also been widely used for inferring evening and nighttime equatorial F region vertical drifts [e.g., *Abdu et al.*, 1981; *Sastri*, 1996; *Batista et al.*, 1996]. Although the ionosonde drifts have well-known limitations, they have long shown clear indications of large longitudinal variations of the F region vertical plasma drifts. This has been largely attributed to the displacement of the geomagnetic and geographic equators and the large differences in the magnetic declination angles and magnetic field strength along the geomagnetic equator.

On the basis of these data, climatological regional models of the equatorial plasma drifts in the Peruvian, Brazilian, and Indian sectors have been developed. *Richmond et al.* [1980] derived an empirical global quiet time model for the F region drifts using

Paper number 1999JA900025.
0148-0227/99/1999JA900025$09.00

incoherent scatter radar observations from Millstone Hill, Arecibo, Saint Santin, and Jicamarca from 1974 to 1977. However, this model is valid only during solar minimum conditions, and at the equator, this model relies entirely on Jicamarca drift observations. In spite of the well-known longitudinal variations, these empirical models have been widely used as input parameters for global low-latitude modeling studies [e.g., *Anderson et al.*, 1987; *Bailey et al.*, 1993].

Over the last decade, satellite observations have increasingly been used to study the global distribution of equatorial F region plasma drifts and, in particular, their longitudinal variability. *Coley et al.* [1990] have used average equatorial vertical plasma drift observations obtained by the low inclination Atmospheric Explorer E (AE-E) satellite from January 1977 to December 1979 and reported largely longitudinally independent diurnal drift patterns, similar to the ones at Jicamarca, for high solar flux equinox conditions. *Fejer et al.* [1995] presented the first detailed study of the global distribution of the equatorial F region vertical plasma drifts using the IDM data from the AE-E satellite also. They showed that the longitudinally averaged satellite drifts are in agreement with the Jicamarca data only during equinox and December solstice. For moderate to high solar flux conditions, the AE-E data indicated large longitudinal variations of the vertical drifts during June solstice. These results are consistent with the vector electric field data obtained during April-August 1988, by the San Marco satellite [*Maynard et al.*, 1995].

In this study, we combine the AE-E data set of *Fejer et al.* [1995] with extensive Jicamarca incoherent scatter radar vertical drift observations from 1968 to 1992 to present the first detailed global empirical model for the equatorial F region vertical drifts that takes into account their diurnal, seasonal, solar cycle, and longitudinal variations. This analytical model, which is generally in good agreement with ionosonde-inferred vertical drifts, should provide considerably more accurate equatorial inputs into global and low-latitude thermospheric, ionospheric, and plasmaspheric models. It can also be combined with our analytical equatorial storm time vertical drift models [*Fejer and Scherliess*, 1997] to provide a global empirical representation of these drifts under different geomagnetic conditions.

In the following sections, we initially describe our Jicamarca and AE-E data sets used to develop the empirical model. Then, we describe the methodology, present our model results, discuss their characteristics and limitations, and compare them with observations.

2. Measurement Techniques and Data

The Jicamarca incoherent scatter radar, located near the magnetic equator near Lima, Peru (12.0°S, 76.9°W, magnetic dip 2°N), has been making F region plasma drift measurements since April 1968. Most of these measurements covered an altitudinal range from about 250 to 600 km, with a height resolution of about 20 km and an integration time of about 5 min. The experimental technique was described by *Woodman* [1970]. The typical uncertainty is about 1-2 m/s during the day and somewhat larger at night, when the signal-to-noise ratio can be significantly smaller, particularly near solar minimum.

The Jicamarca drift data have been extensively used for investigations of equatorial vertical plasma motions [e.g., *Fejer et al.*, 1979, 1989, 1991]. These studies have generally used drift averages from about 300 to 400 km where the signal-to-noise ratio is highest and the vertical drifts do not change much with altitude. The latest version of the average quiet time Jicamarca plasma drifts was presented by *Fejer et al.* [1991]. They used 367 days of observations from 1968 to June 1988 to derive 4-month seasonally averaged drifts for low, moderate, and high solar flux conditions. In the present study, we used 502 days of observations from 1968 to April 1992. Figure 1 shows a scatterplot of the seasonal Jicamarca drift observations used in this study for low, medium, and high solar flux conditions. Figure 1 shows excellent data distribution for all seasons and local times, except for low solar flux early morning solstitial periods.

The low-latitude AE-E satellite (inclination 19.76°) made ionospheric measurements from the end of 1975 through June 1981. Here we have used the data set of *Fejer et al.* [1995], which comprises vertical plasma drift observations obtained by the ion drift meter (IDM) from January 1977 to December 1979, when the satellite was in nearly circular orbits with the altitude increasing from 230 to 470 km. This data set consists of 15-s-averaged IDM drift observations extracted from the unified abstract (UA) files. The details of the IDM are discussed by *Hanson and Heelis* [1975]. The relative and absolute precisions of the drift measurements are about 2 and 7 m/s, respectively. *Fejer et al.* [1995] discussed the limitations of this data set for equatorial vertical plasma drift studies and a number of criteria used to minimize the effects of instrumental biases.

In general, the vertical ion velocity has drift components perpendicular and parallel to the geomagnetic field, but at the dip equator it essentially results from the $\mathbf{E}\times\mathbf{B}$ drift due to a zonal electric field. *Fejer et al.* [1995] have shown that the seasonally and longitudinally averaged diurnal patterns of the vertical drifts are essentially unchanged for dip latitude ranges up to $\pm$ 7.5°. We have also used this relatively large dip latitudinal range to maximize the number of available drift observations, without introducing a bias of the electrodynamic drifts by field-aligned motions outside the day-to-day variability of the data.

Figure 2 shows a scatterplot of the satellite drift observations used in this study for low ($S_a \leq 130$) and high ($S_a \geq 130$) solar flux conditions. Figure 2 shows good data coverage for all seasons and solar flux conditions, except for low solar flux December solstice after-

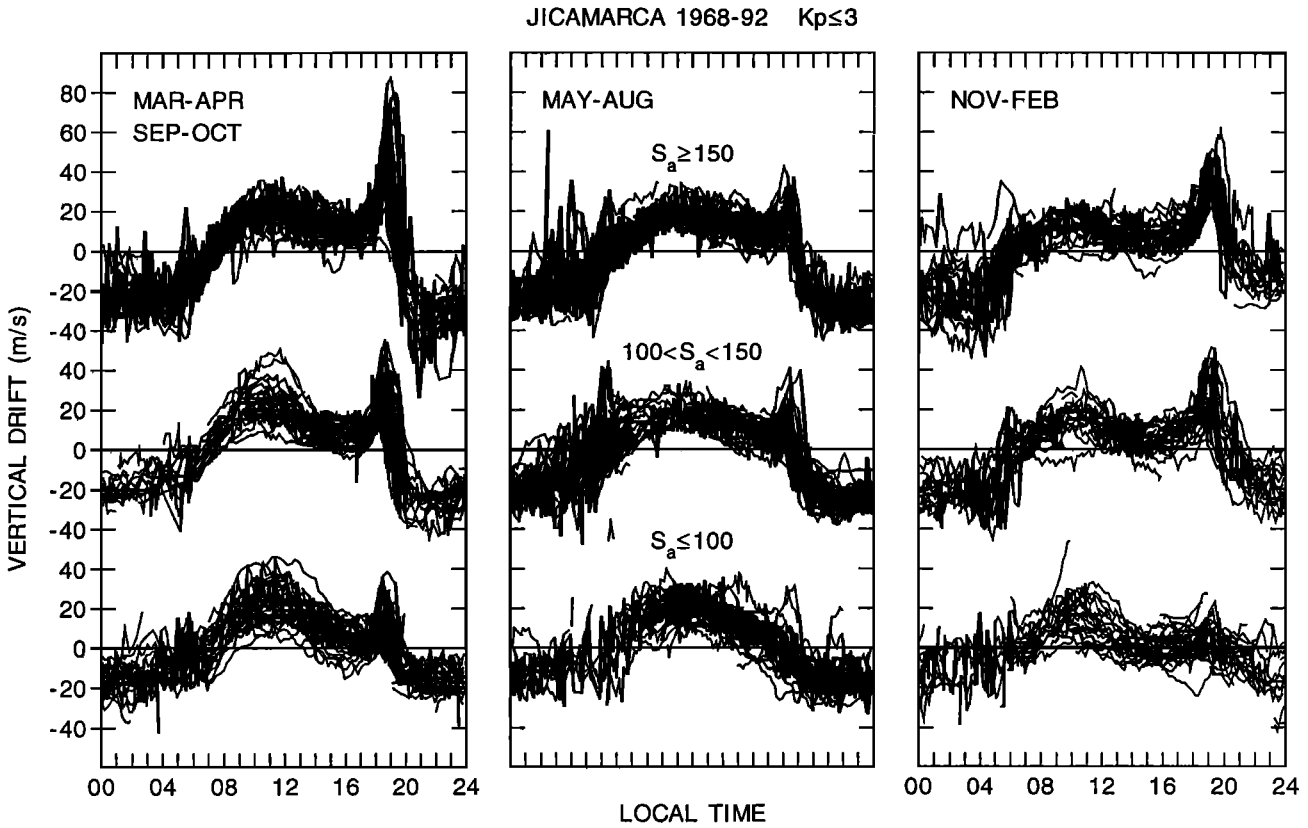

Figure 1. Scatterplot of the 1968-1992 Jicamarca quiet time vertical drifts for low, medium, and high solar flux conditions.

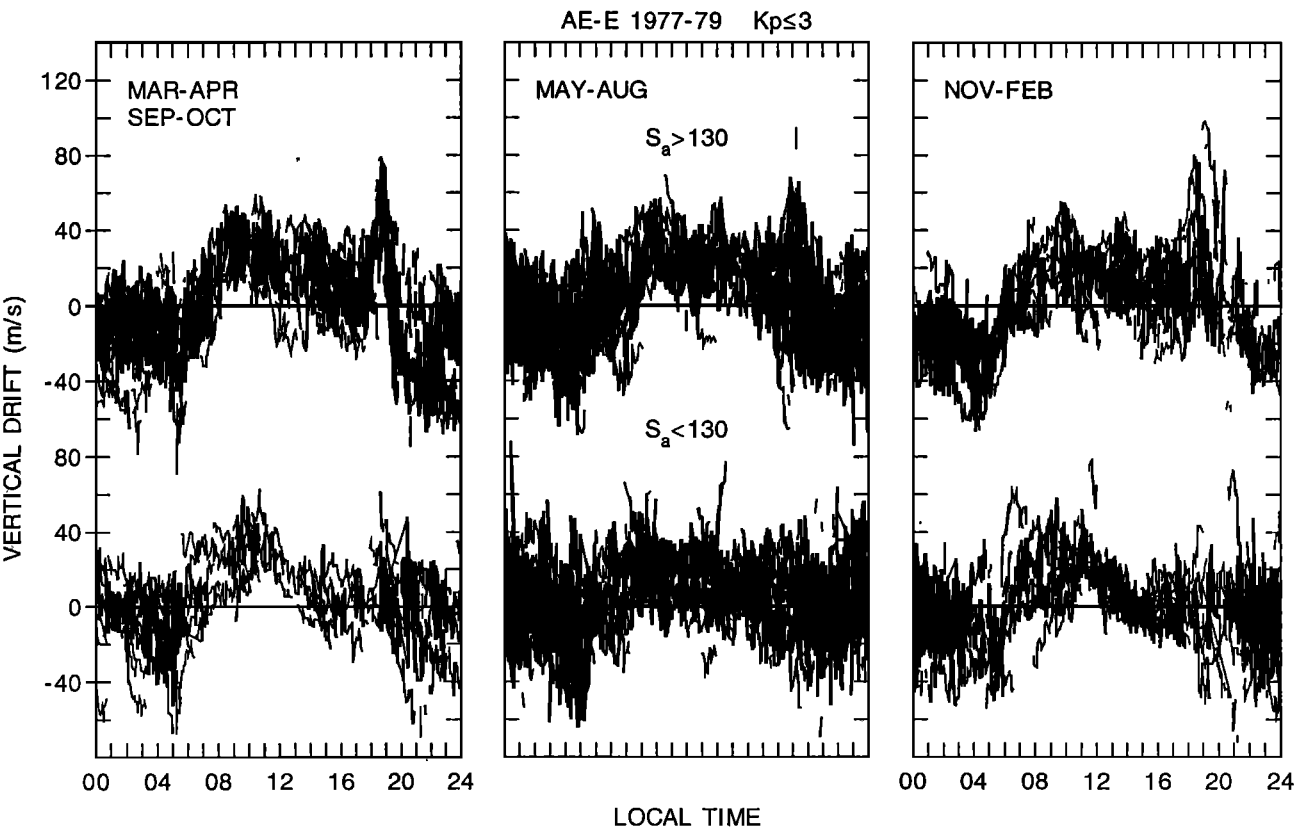

Figure 2. Scatterplot of the 1977-1979 AE-E quiet time vertical drifts for low and high solar flux conditions.

noon periods. A detailed description of the longitudinal distribution of the high solar flux satellite data can be found in the work of *Fejer et al.* [1995].

3. Model Development and Description

In this section, we describe our satellite-radar equatorial vertical plasma drift model. This empirical model incorporates local time, longitudinal, seasonal, and solar cycle variations of the drift velocities. Variations due to geomagnetic activity have not been addressed in this study but can, in principle, be incorporated in the model by using, for example, the results of *Fejer and Scherliess* [1997]. Altitudinal variations of the equatorial vertical drifts [e.g., *Pingree and Fejer*, 1987; *Coley and Heelis*, 1989; *Fejer et al.*, 1996] are also not included in the current model. As shown in Figures 1 and 2, the equatorial drifts show considerable day-to-day and shorter-term variability, but these effects will not be investigated here.

In a straightforward approach, we could have developed our empirical drift model by simultaneously fitting all satellite and radar vertical drift observations using appropriate functions, and suitable weighting factors to these two data sets. In this approach, the longitudinal dependence of the drifts would be given mainly by the satellite data, and a combination of both data sets would have determined the model drifts in the Peruvian sector. However, as shown in Figure 2 (and also Figure 5 of *Fejer et al.* [1995]), the satellite database shows relatively sparse data coverage in some longitudinal sectors and also during some seasons. In addition, an observed discrepancy between the nighttime satellite and radar drift observations has yet not been resolved [*Fejer et al.*, 1995]. As a result, the longitudinally averaged drifts at different universal times do not generally maintain conservative electric fields. Therefore we have chosen to use information from the Jicamarca radar drift observations also in other longitudinal sectors and to constrain the model drift amplitudes so that the curl-free condition is nearly satisfied at all times.

In essence, we have spread the radar data over a grid of longitudes along the geomagnetic equator and combined them with the satellite data using separate weighting factors during the day and during the night. On the basis of these data, we have initially developed seasonal vertical drift models for low and high solar flux conditions, and then constrained the model drift amplitudes using the curl-free condition of the electric field. Finally, the separate seasonal and solar cycle models were combined into one single model representation. In the following sections, we will describe these steps in more detail.

3.1. Data Preparation

The satellite and radar data sets have been grouped separately into seasonal bins representing June solstice (May-August), December solstice (November-February) and equinox (March-April, September-October) conditions and two levels of 10.7-cm solar activity yielding average solar flux values of about 90 and 180 (in units of 10^{-22} $Wm^{-2}Hz^{-1}$), respectively. Only data taken during geomagnetically quiet conditions ($Kp \leq 3.0$) have been used. Since the daytime equatorial vertical drifts are essentially independent of solar activity [e.g., *Fejer et al.*, 1991, 1995], we have enhanced the available data points in each bin by combining the satellite low and high solar flux data in the 0600 to 1500 LT sector.

Initially, we have spread the radar data over a grid of longitudes (grid size 10°) spanning around the entire globe. Longitudinal effects are most pronounced during the solstices. Therefore, as a first-order correction, we have switched the seasonal patterns from one season to the other when the dip equator crossed the geographic equator. In a transition zone, when the dip equator was close to the geographic equator, we have used a combination of both June and December solstice data. Such a relatively simple extension of the Jicamarca drift data over the entire equatorial region has frequently been used with reasonable success in past modeling studies when only the Jicamarca data were available (D. Anderson, private communication, 1994). For easier computation, these data were averaged in 1/2-hour LT bins and also in 30° overlapping longitudinal bins spaced by 10°.

Fejer et al. [1995] showed that the high solar flux (1978-1979) AE-E vertical drift averages from the American sector are in good agreement with the more accurate Jicamarca data during the day, but differ significantly from about 2100 to 0300 LT, particularly during June solstice. The reasons for these differences are not understood [*Fejer et al.*, 1995]. Therefore, to combine the different drift observations individual weighting factors have been introduced. From about 0400 to 2100 LT, when the satellite data are most reliable, a weight of about 75% was given to the satellite data. From about 2100 to 0400 LT, however, we have decreased the weight of the satellite data to only about 25%. In some local time/longitude sectors, this weighting factor has been modified to give more satisfactory results, in particular to avoid small scale temporal and spatial oscillations. Without an exact knowledge of the cause of the discrepancies between the satellite and the radar data, it should be clear that our choice of weighting factors is somewhat subjective. In a later step, we will use the curl-free condition of the electric field to obtain a more objective representation of the vertical drifts. We will also further increase the weight of the Jicamarca radar data in the Peruvian sector to give a better agreement between the model and the radar data. Alternatively, we could have used weighting factors based on the standard deviation of the satellite and radar data in each local time/longitude bin, but this would have significantly affected regions of large temporal and spatial gradients, which are often of particular interest.

3.2. Derivation of the Model Drifts

We describe the local time (t) and longitudinal (φ) dependences of the vertical drifts for each season and solar flux interval by products of univariate normalized cubic-B splines of order four, $N_{i,4}(t)$ and $N_{j,4}(\varphi)$:

$$v(t,\varphi) = \sum_{i=1}^{N} \sum_{j=1}^{4} a_{i,j} N_{i,4}(t) N_{j,4}(\varphi). \quad (1)$$

These basis functions are nonvanishing over limited intervals and add up to one at all local times and longitudes [e.g., *DeBoor*, 1978]. They are ideally suited to model the equatorial vertical drifts, with their smooth daytime and nighttime features and rapid changes near the terminators, by a proper placement of the mesh of nodes. Four longitudinal nodes were placed in equally spaced longitudinal intervals at 0, 90, 180, and 270°. The number and placement of the local time nodes for each season and solar flux interval were individually chosen to account for the large variability in the average vertical drift profiles from one condition to another. For example, near dusk, and in particular at the time of the prereversal velocity enhancement, the solar maximum data show considerably larger local time gradients than the solar minimum data. Consequently, a larger number of basis functions was needed to account for these rapid changes in the solar maximum drifts. We chose 9 basis functions for the solar minimum data and 12 functions for the maximum data with a denser mesh of the local time nodes around dawn and dusk. Certainly, we could have used the same higher density mesh for all geophysical conditions, but this would have introduced additional freedom to the fitting, even when the vertical drifts are relatively constant spatially and/or temporally. In a later step, we will actually use this approach to obtain a single model representation for all seasons and solar flux conditions. The coefficients $a_{i,j}$ in (1) were determined by a least squares fit to the binned data and constrained to make the fit periodic in 24 hours and 360°.

In the next step, we have used the curl-free nature of the electric field to constrain the drift amplitudes and finally combined the individual seasonal and solar cycle models to obtain our final quiet time model. For this purpose, we have computed quarter-hourly seasonal drift patterns for each 10° longitude and for low and high solar flux conditions. As mentioned above, the vertical plasma drift at the geomagnetic equator is directly driven by the zonal component of the electric field. At any given time, this electric field component must be irrotational, and thus the line integral of this electric field along the equator is constrained to be zero; i.e.,

$$\oint \mathbf{E} d\varphi = \oint B v_z d\varphi = 0, \quad (2)$$

where B denotes the equatorial magnetic field strength, which varies between about 0.22 and 0.34 G along the geomagnetic equator. We have introduced this constraint for each quarter-hourly UT by first multiplying the drift velocities on a 5° longitudinal grid by the appropriate magnetic field strength B, which was obtained from the International Geomagnetic Reference Field (IGRF) [*Bilitza et al.*, 1992], and then integrated the resulting zonal electric field component along the geomagnetic equator. The resulting quarter-hourly velocity offsets were used to shift the drift amplitudes to maintain near-conservative electric fields. Since the daytime satellite drift observations are more reliable than the nighttime measurements, we have used the full shift during the night, but only 50% during the day. The remaining displacement of the drifts from the ideal irrotational electric field is less than 2 m/s at all quarter-hourly periods.

To increase the accuracy of the model in the Peruvian sector, we have again utilized the Jicamarca observations by giving them a weight of 50%, but this time restricted to the Peruvian sector. To spatially restrict the effect of the Jicamarca data to a region of approximately ± 25° centered around the longitude of Jicamarca, we increased the longitudinal resolution of our model in the American sector by introducing additional nodes.

Finally, a simultaneous fit has been performed and the drifts are expressed as

$$v(t,\varphi,d,S_a) = \sum_{i=1}^{13} \sum_{j=1}^{8} \sum_{k=1}^{6} a_{i,j,k} f_k N_{i,4}(t) N_{j,4}(\varphi) \quad (3)$$

with

$$\begin{aligned} f_1 &= 1 && \text{May-August} \\ f_2 &= 1 && \text{November-February} \\ f_3 &= 1 && \text{March-April, September-October} \\ f_4 &= f_1 && (S_a - 140) \\ f_5 &= f_2 && (S_a - 140) \\ f_6 &= f_3 && (S_a - 140) \end{aligned}$$

Here again, t denotes local time, φ is geographic longitude, d is day of the year, and S_a is the daily 10.7-cm solar activity. Outside their above defined limits, the functions f_1 to f_3 are set to zero. The coefficients $a_{i,j,1}$ to $a_{i,j,3}$ determine the basic seasonal patterns of the equatorial vertical drifts for a solar flux of 140 and the coefficients $a_{i,j,4}$ to $a_{i,j,6}$ represent the linear variations of the vertical drifts with the phase of the solar cycle. The local time and longitudinal B-spline functions are shown in Figure 3. As mentioned above, during some geophysical conditions (e.g., low solar flux) a smaller number of basis functions would have been sufficient, but the advantages of one unified model description certainly outweigh the convenience of slightly fewer model coefficients. This model description is also relatively easily upgradable when more satellite drift data become available. For example, our simple functions

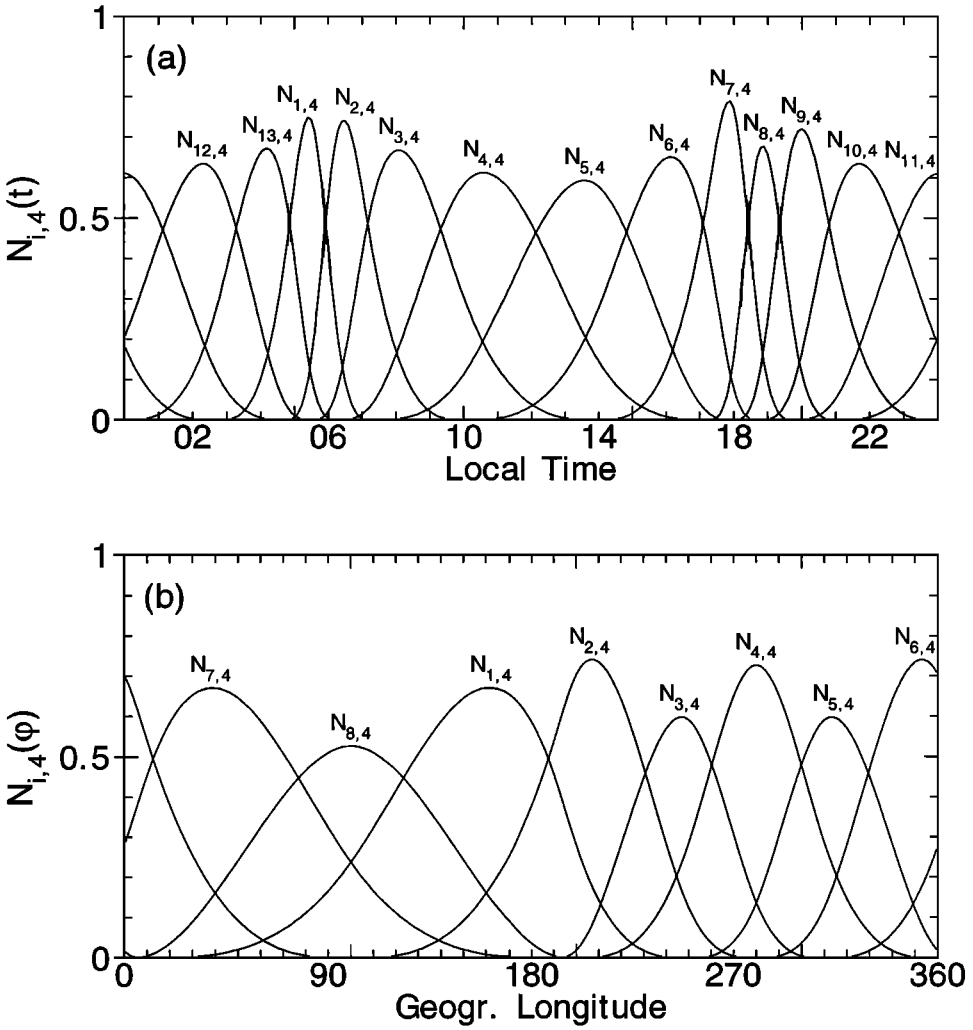

Figure 3. Basis functions for the (a) local time and (b) longitudinal dependence of the equatorial vertical drifts.

f_1 to f_3 could be replaced by sinusoidal functions to describe the seasonal drift variations more realistically. In addition, in future studies, data from ground-based observations other than Jicamarca, e.g., ionosonde measurements, could be incorporated in the model by a proper placement of additional longitudinal basis functions. Of course, these measurements should be fully validated first.

Finally, a simple linear interpolation scheme over a range of ± 15 days was employed for the transition from one season to the other. This interpolation provides a reasonably realistic transition between seasons.

In summary, we have derived a global empirical model for the quiet time F region equatorial vertical drifts. Input parameters for this analytical model are continuous values of local time, longitude, $F10.7$-cm solar flux, and day of the year. The longitudinal and temporal resolution of our model is about 30° and 1/2 hour, respectively. In the near future, we intend to incorporate this model into a global ionospheric electric field model, which will be derived using data from all mid-latitude and low-latitude incoherent scatter radars and also from satellite measurements. This model will be accessible through the NCAR CEDAR data base in the near future. However, for the time being, a copy of our present model can be obtained from the authors.

4. Results and Discussion

In this section, we will initially validate the model results by comparing them with average AE-E and Jicamarca observations and then discuss the characteristics and limitations of the model. Finally, we will compare our model predictions with other observations.

4.1. Model Validation

A comparison of the model results with binned and averaged AE-E vertical drift observations for low (1977-1978) and high (1978-1979) solar flux conditions is shown in Figures 4 and 5, respectively. The average solar flux values during these periods were between 90 and 110, and 170 and 190, respectively. The data have been grouped in four overlapping longitudinal bins, largely representative of the African-Indian

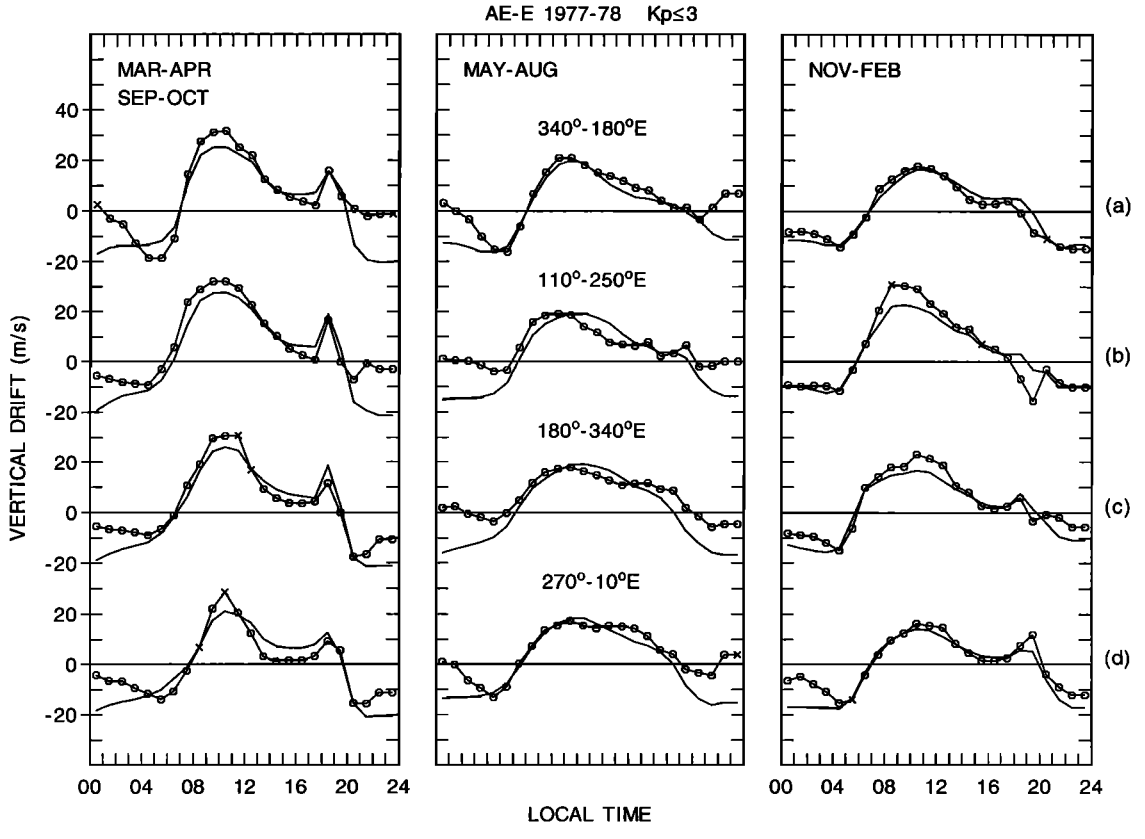

Figure 4. Comparison of the model predictions (solid curves with no symbols) with AE-E vertical drift observations in four longitudinal sectors and low solar flux conditions. The asterisk denotes averages from less than 30 data points.

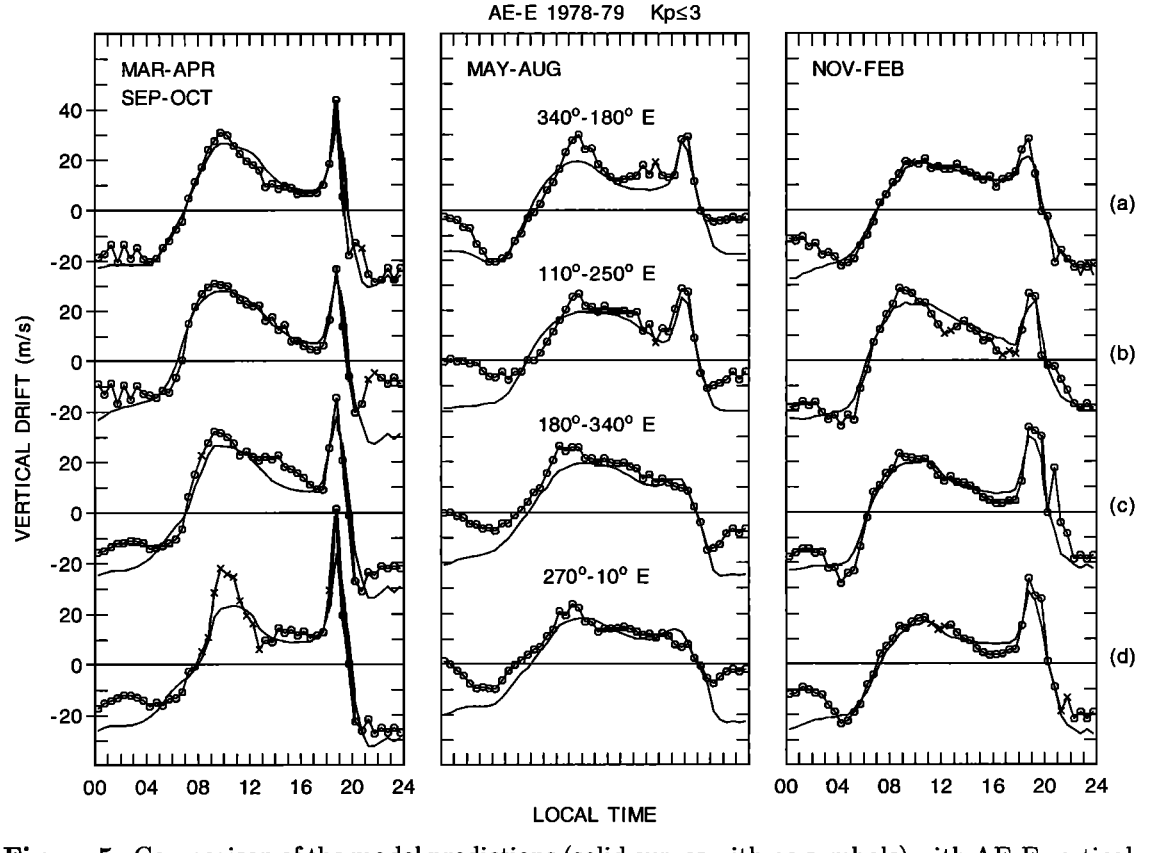

Figure 5. Comparison of the model predictions (solid curves with no symbols) with AE-E vertical drift observations in four longitudinal sectors and high solar flux conditions. The asterisk denotes averages from less than 15 data points.

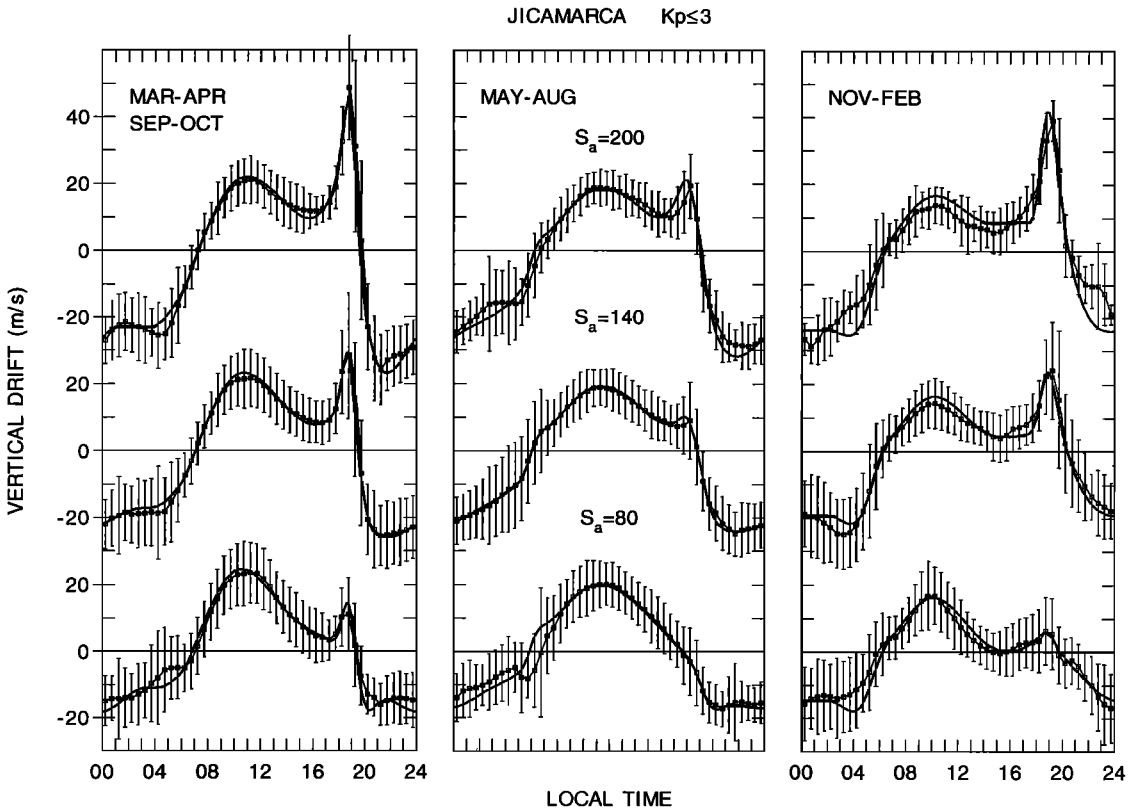

Figure 6. Comparison of the model predictions with average drift patterns obtained from the Jicamarca drift observations for equinox, June solstice, and December solstice conditions for low, medium, and high solar flux periods.

(Figures 4a and 5a), the Asian-Pacific (Figures 4b and 5b), the Pacific-American (Figures 4c and 5c), and the American-Atlantic (Figures 4d and 5d) sectors, and averaged in hourly and half-hourly solar local time bins for low and high solar flux conditions, respectively. The model drifts have been calculated for each data point and binned and averaged in the same way as the observations. As expected, the empirical daytime drifts are generally in good agreement with the average satellite drift values, except in the 0800-1100 LT sector, where the model often underestimates the average satellite drifts. However, in this local time sector, the model drifts over Jicamarca are in excellent agreement with the average radar observations. The largest discrepancies occur during June solstice nighttime period where, as mentioned above, the satellite measured unrealistically small nighttime downward drifts. During equinox conditions, these nighttime discrepancies are also observed, although they are less noticeable. The model and satellite reversal times are generally in excellent agreement, except in the Pacific-American sector during periods of low solar flux when the satellite drifts show a reversal time approximately 1.5 hours later than the model. In this sector, however, we will show that the model reversal times are in excellent agreement with the average Jicamarca data.

Figure 6 shows a comparison of the model results over Peru with seasonally averaged Jicamarca radar drifts. The radar data were averaged in half-hourly bins and three levels of solar activity corresponding to approximately 80, 140, and 200 solar flux units during all seasons. The vertical bars indicate the scatter in the radar data and not the error on the measurements. The model results are shown for the longitude of Jicamarca (76.87° W) and for the average solar flux values of the radar observations. The model and radar data are in very good, although not perfect, agreement. Some of the discrepancies result from our assumed linear solar cycle dependence which, during solar minimum June solstice early morning conditions, results in noticeable differences between the model predictions and the average radar observations. The observed discrepancies between the average December solstice radar observations and the model drifts are most likely due to the large variations observed in the vertical drift patterns during this 4-month period [*Fejer et al.*, 1995]. Most of the low solar flux December solstice data were measured during January, whereas most of the high flux data were obtained during December. Our model, however, should best represent an average drift pattern over this 4-month period.

4.2. Solar Cycle Variations

Figure 7 shows the average seasonal variations of the vertical drifts for a change in the solar flux by 100 units in four longitudinal sectors. In each sector, the drift

variations have been derived from (3) by subtracting the model responses for S_a=100 from the responses for S_a=200 in 10° longitudinal steps. Finally, the residuals have been averaged over the corresponding longitudinal bins. As expected, only small variations are observed during the day, except in the American sector during December solstice conditions. It is not clear if this large daytime solar cycle dependence is entirely realistic or a result of the Jicamarca radar data distribution during this season, as mentioned above. Near dusk, at the time of the prereversal velocity enhancement, strong variations in the vertical drifts with the phase of the solar cycle are observed with typical values of 20-30 m/s for a 100 unit change in the solar flux index. During nighttime, somewhat smaller values (5-15 m/s) are found. The largest variation with the solar cycle is observed in the Pacific region during June solstice conditions with an increase in the prereversal velocities by more than 40 m/s for an increase in 100 solar flux units. The solar cycle dependence in the Western American sector is in excellent agreement with *Fejer et al.* [1991], although important nonlinear features, e.g., the saturation of the June solstice high solar flux drift values [*Fejer et al.*, 1989], are neglected in our linear model.

It is important to note that the satellite altitude increased by about 240 km from 1977 to 1979, and therefore some of the apparent solar cycle dependence could also result from altitudinal variations of the equatorial vertical drifts. Clearly, additional data are needed to clarify this solar cycle dependence.

4.3. Longitudinal Variations

The longitudinal variations of the equatorial vertical drift patterns obtained from our empirical model for low (S_a=90) and high (S_a=180) solar flux conditions during June solstice, December solstice, and equinox conditions are presented in Figure 8.

The low solar flux equinoctial evening drifts show only small longitudinal variations and display prereversal velocity enhancements with amplitudes between about 15 and 20 m/s. Near solar minimum, the prereversal velocity enhancement is not observed during June solstice, and is only developed in the American sector during December solstice, where it reaches amplitudes between about 5 and 10 m/s.

The solar minimum evening reversal times are fairly independent of longitude during equinox and June solstice when they occur at about 1930-1945 LT and 1800

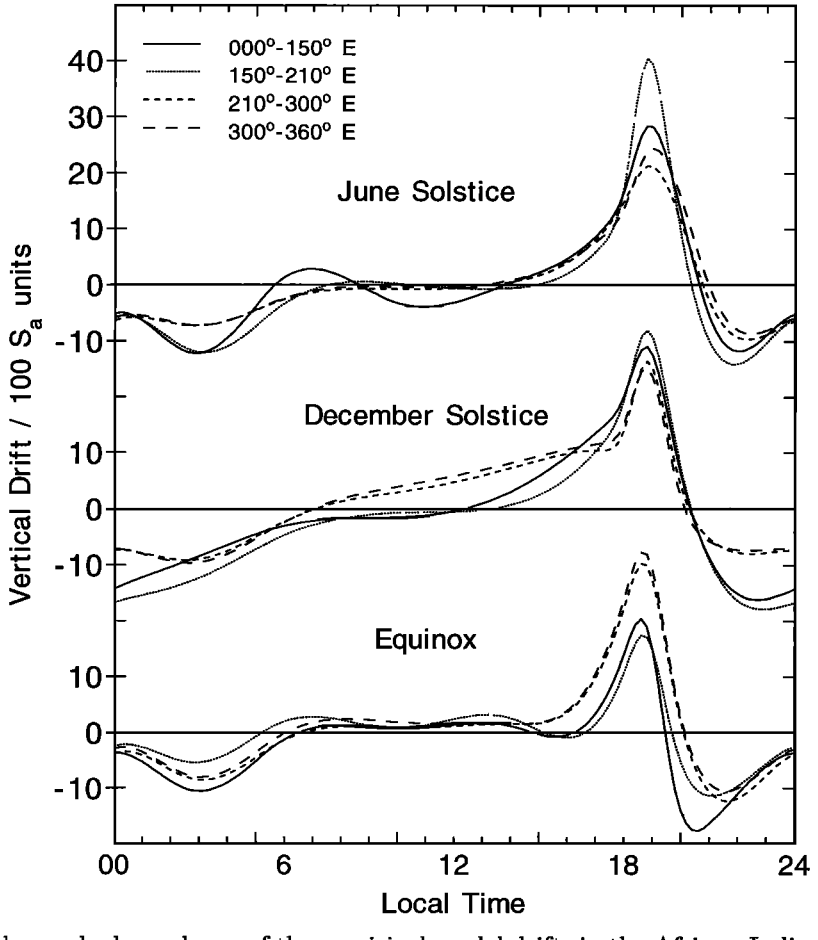

Figure 7. Solar cycle dependence of the empirical model drifts in the African-Indian (0°-150° E), Pacific (150°-210° E), Western American (210°-300° E), and Brazilian (300°-360° E) equatorial regions.

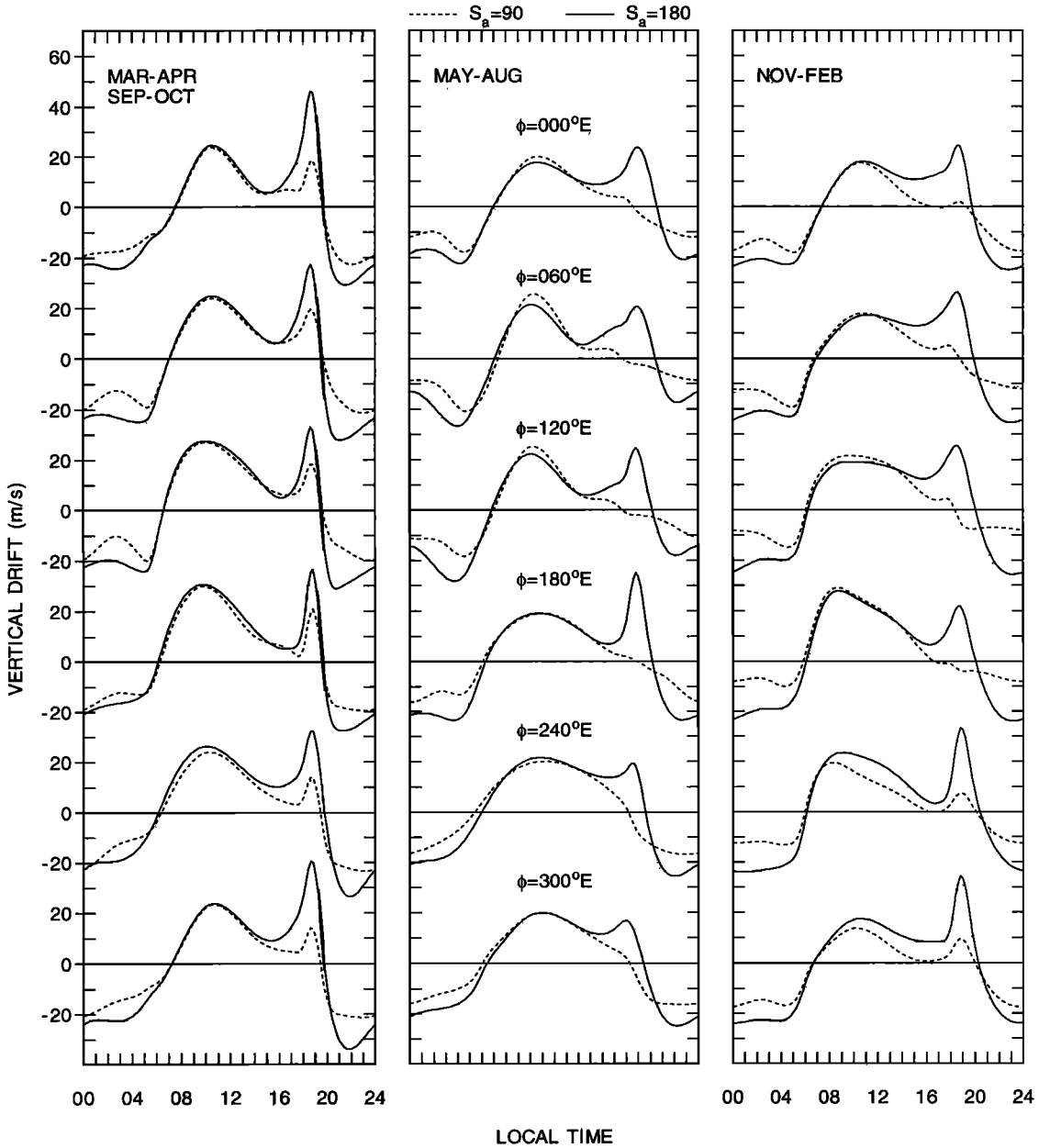

Figure 8. Empirical model results in six longitudinal sectors for low (dashed) and high (solid line) solar flux conditions.

LT, respectively. As shown earlier, these reversal times are in excellent agreement with Jicamarca radar data (Figure 6) but differ significantly from the average satellite data during June solstice in the American sector (Figure 4). The December solstice evening reversal times show large variations from about 2000 LT in the American sector to 1830 LT in the Indian sector and 1600 LT in the Pacific sector. However, in the latter sector, as well as in the Atlantic-African sector, the drift amplitudes in the late afternoon/evening period are only about 1-3 m/s and small dc offsets can consequently affect these reversal times dramatically.

The morning reversal times and the daytime drifts exhibit only small variations with the phase of the solar cycle (see also Figure 7). During June solstice, the morning reversal times vary between about 0515 LT in the Pacific-American sector and about 0715 LT in the African-Indian sector. These reversal times are in good agreement with the satellite data but are about one hour earlier than shown by the Jicamarca radar data (the radar data are rather sparse near the morning reversal time for low flux conditions). During equinox and December solstice, the morning reversal times occur earliest in the Pacific sector and latest in the Atlantic-African sector.

The daytime drifts have largest amplitudes (about 25-30 m/s) between about 0900 and 1100 LT in the Indian sector during June solstice and near the Pacific sector

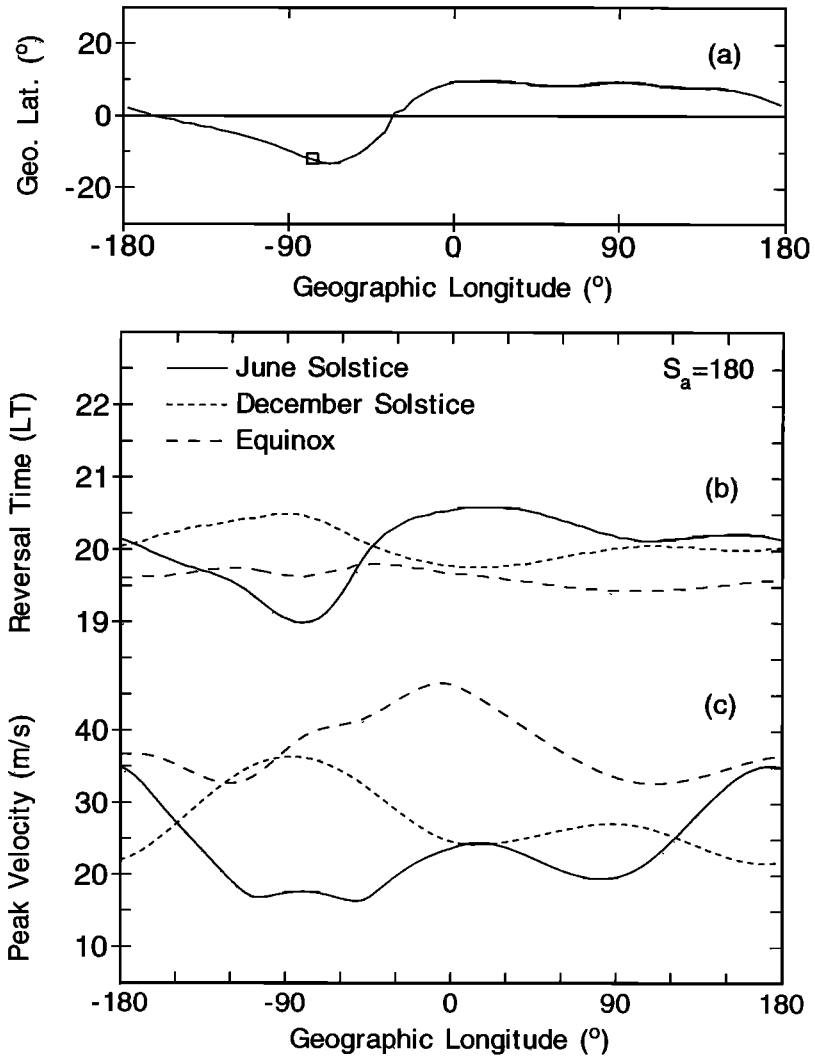

Figure 9. Longitudinal variation of the (a) location of the dip equator, the model predictions for the (b) evening reversal time, and (c) evening peak velocities for the three seasons and high solar flux conditions.

during Equinox and December solstice. The morning and early afternoon drifts are largely solar flux independent.

The late afternoon/evening solar maximum vertical drifts exhibit large longitudinal variations, particularly during June solstice. In this case, the prereversal peak velocities and the evening reversal times can be accurately determined. Figure 9 shows the longitudinal variation of the dip equator and the empirical evening reversal times and prereversal peak velocities for the three seasons for a solar flux index of 180. The peak velocities exhibit large longitudinal variations. The equinoctial peak drifts have values of about 45 m/s in the Brazilian-African sector, but reach only about 35 m/s in the Pacific sector. The solstitial data show significant variations between the American and Pacific sectors. The June solstice peak drifts maximize in the Pacific region with drift amplitudes of up to 35 m/s, whereas the December solstice velocities maximize in the American sector with comparable magnitudes. The evening reversal times also exhibit large longitudinal variations, particularly near June solstice. Here we find the earliest reversal times at about 1900 LT in the West American sector. In this sector, the December solstice data reverse latest at about 2030 LT. The relatively large number of drift observations in the June solstitial evening sector (see Figure 2) allows for a detailed comparison of the empirical reversal times with satellite drift observations in this sector, which is presented in Figure 10. The sharp decrease in the empirical reversal times from the eastern to the western American sector is in good agreement with the satellite data, although these measurements indicate a systematically later ($\approx$ 15 min) reversal time. Also, note the good agreement of the empirical and measured prereversal peak velocities. *Fejer et al.* [1991] reported large longitudinal variations in

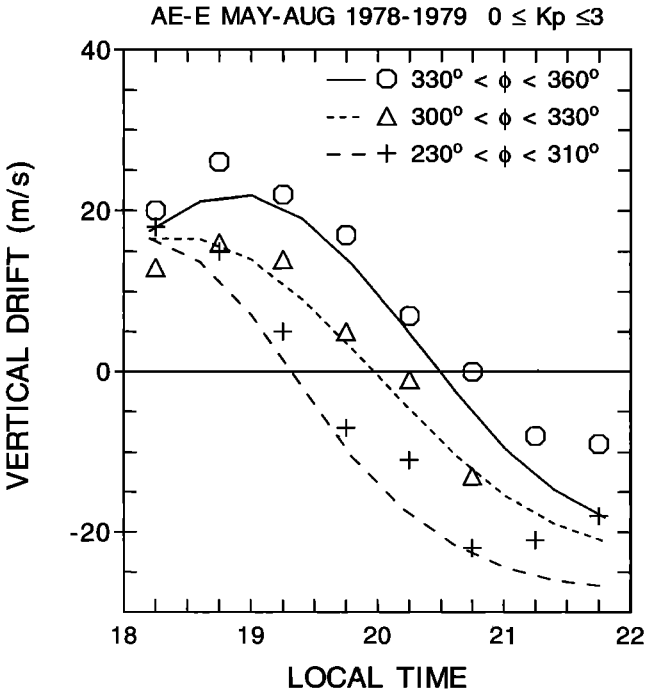

Figure 10. Longitudinal variation of the empirical (solid and dashed lines) and satellite (symbols) equatorial vertical drifts in the afternoon-evening sector for May-August moderate to high solar flux and magnetically quiet conditions. Here Φ denoted east longitude.

the evening reversal times determined from ionosonde measurements in four longitudinal sectors. Our results are in good agreement with these earlier results.

4.4. Comparison With Other Observations

Figure 11 shows a comparison of the empirical model drifts with vertical model drifts derived from ionosonde observations over Fortaleza, Brazil (4°S, 38°W, magnetic dip 7.5°S) [*Batista et al.*, 1996]. These results show generally good agreement between these two models except for June solstice solar maximum conditions. However, as pointed out by *Maruyama* [1996], thermospheric neutral winds can play an important role on the vertical drifts over Fortaleza as a result of the large declination over this station.

Figure 12 shows a comparison of our model drifts with vertical drifts obtained by the ALTAIR incoherent scatter over Kwajalein (9.4°N, 167.5°E, magnetic dip 7.9°N) [*Sultan*, 1994, 1996] over a 25-day period during the July-August 1990, CRRES-at-Kwajalein campaign. These data, which are averaged over 15-min periods and correspond to an average solar flux index of approximately 200, are in excellent agreement with our model results.

Equatorial vertical drifts have also been derived from ionosonde and HF radar observations over Trivandrum, India (8.3°N, 77°E) [*Hari and Murthy*, 1995; *Balan et al.*, 1992]. Our empirical model results are in good agreement with the ionosonde results, but underestimate the HF radar evening prereversal velocities by about 10 m/s. However, their study is based on only eight consecutive days of HF radar observations during March-April 1988 when the vertical drifts exhibited large day-to-day variability. Moreover, the Trivandrum drifts differ significantly from drift observations made at Kodaikanal [*Sastri*, 1996], which is located only 2° to the north. Therefore it is not clear how well our model results agree with these ground-based measurements.

Deminov et al. [1988] have inferred solar maximum vertical drift velocities using F region peak electron densities measured by the Interkosmos-19 (IK-19) satellite near 1400 LT during December and June 1980. Their results suggest that the upward drifts from December are larger than those from June, except for the 180°-300°E longitudinal sector, in agreement with our results. *Maynard et al.* [1995] have used electric field measurements from the San Marco D satellite from April to September 1988 to infer the morphology of the equatorial vertical plasma drifts during periods of quiet to moderate solar activity. Their results show larger daytime upward drifts in the Indian sector than in the Peruvian sector during June solstice, in agreement with our results, although their longitudinal daytime variations are significantly larger than suggested by our model results. The San Marco D data set during equinox is too small to determine the longitudinal variations of the vertical drifts. However, their longitudinally averaged equinoctial daytime drifts maximize in the 1100-1500 LT sector, whereas our results, based on significantly larger data sets, suggest daytime peak velocities between about 0900-1100 LT. Additional satellite and ground-based drift measurements would be highly desirable for improving our empirical model.

5. Summary and Conclusions

Extensive incoherent scatter radar observations from Jicamarca and IDM measurements on board the low inclination AE-E satellite were used to develop the first global empirical ionospheric vertical plasma drift model. This model incorporates the daily, seasonal, solar cycle, and longitudinal variations of the equatorial vertical drifts and provides a reasonably realistic description of the equatorial vertical drifts. The model results are in good agreement with other ground-based vertical drift observations over the Brazilian, Indian, and Pacific regions. The equatorial F region drifts show largest longitudinal variations during the solstices and smallest during equinox. Some important features, such as the altitudinal variation of these drifts, nonlinear solar cycle variations, and differences between the vernal and autumnal drift velocities, which are observed in Jicamarca data [*Scherliess*, 1997], can be included when additional data become available. We also intend, in the near future, to incorporate our current model into a global ionospheric electric field model, which will be accessible through the NCAR CEDAR database. A copy of the current model can be obtained from the authors.

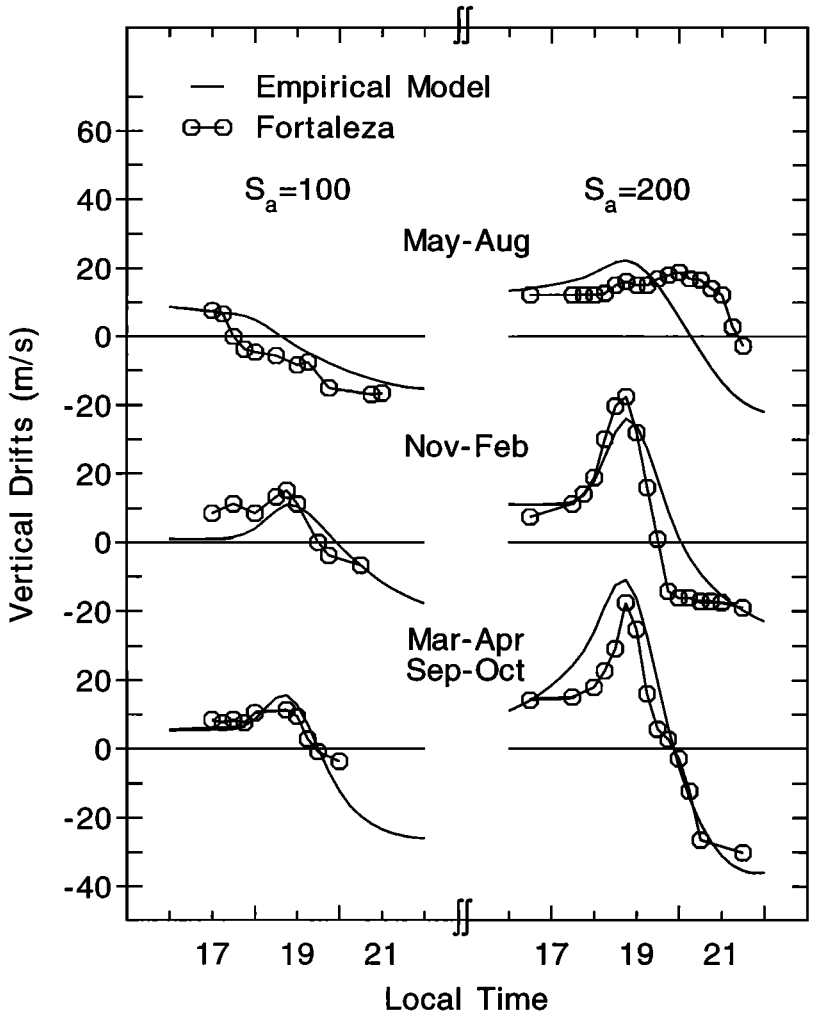

Figure 11. Comparison of the model predictions in the Brazilian sector with Fortaleza ionosonde model drifts.

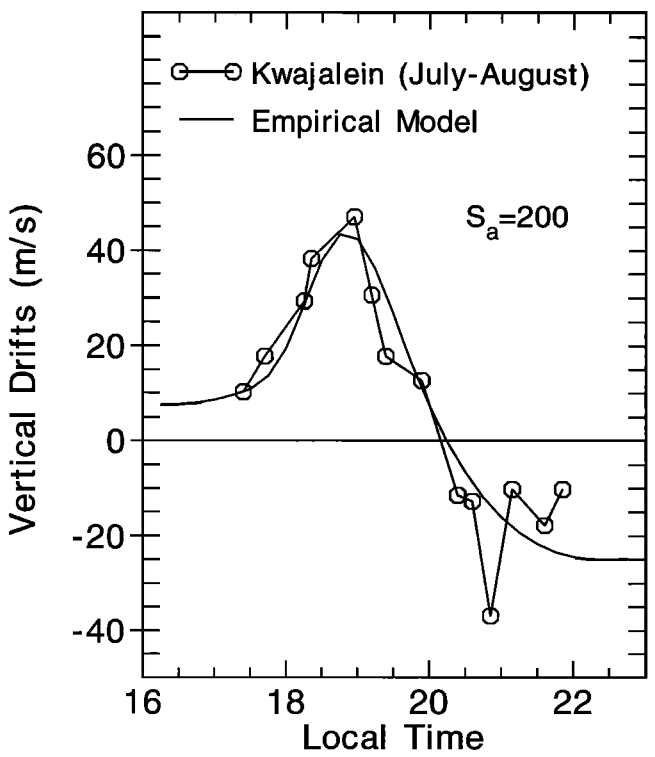

Figure 12. Comparison of the model predictions in the Kwajalein sector with results from the ALTAIR incoherent scatter radar [adapted from *Sultan*, 1994].

Acknowledgments. We thank E. de Paula for help with the satellite data. This work was supported by the Aeronomy Program, Division of Atmospheric Sciences, of the National Science Foundation through grants ATM--9714677 and ATM-9731704 and by the National Aeronautics and Space Administration through grant NAG5-4469. The Jicamarca Radio Observatory is operated by the Instituto Geofisico del Peru, with support from the National Science Foundation.

Janet G. Luhmann thanks William Robin Coley and J. Hanumath Sastri for their assistance in evaluating this paper.

References

Abdu, M. A., J. A. Bittencourt, and I. S. Batista, Magnetic declination control of the equatorial *F* region dynamo electric field development and spread *F*, *J. Geophys. Res., 86,* 11,443-11,446, 1981.

Anderson, D. N., M. Mendillo, and B. Herniter, A semi-empirical low-latitude ionospheric model, *Radio Sci., 22,* 292-306, 1987.

Bailey, G. J., R. Sellek, and Y. Rippeth, A modeling study of the equatorial topside ionosphere, *Ann. Geophys., 11,* 263-272, 1993.

Balan, N., B. Jayachandran, R. Balachandran Nair, S. P. Namboothiri, G. J. Bailey, and P. B. Rao, HF Doppler observations of vector plasma drifts in the evening *F*-region at the magnetic equator, *J. Atmos. Terr. Phys., 54,* 1545-1554, 1992.

Batista I. S., R. T. deMedeiros, M. A. Abdu, J. R. deSouza, G. J. Bailey, and E. R. dePaula, Equatorial ionospheric vertical plasma drift model over the Brazilian region, *J. Geophys. Res., 101,* 10,887-10,892, 1996.

Bilitza, D., Solar-terrestrial models and application software, *Planet. Space Sci., 40,* 541-579, 1992.

Coley, W. R., and R. A. Heelis, Low-latitude zonal and vertical ion drifts seen by DE 2, *J. Geophys. Res., 94,* 6751-6761, 1989.

Coley, W. R., J. P. McClure, and W. B. Hanson, Equatorial fountain effect and dynamo drift signatures from AE-E observations, *J. Geophys. Res., 95,* 21,285-21,290, 1990.

DeBoor, C. A., A practical guide to splines, *Appl. Math. Sci.,* vol. 27, 1978.

Deminov, M. G., N. A. Kochenova, and Y. S. Sitnov, Longitudinal variations of the electric field in the dayside equatorial ionosphere, *Geomagn. Aeron., 28,* 57-60, 1988.

Fejer, B. G., The electrodynamics of the low-latitude ionosphere: Recent results and future challenges, *J. Atmos. Solar Terr. Phys., 59,* 1465-1482, 1997.

Fejer, B.G., and L. Scherliess, Empirical models of storm-time equatorial zonal electric fields, *J. Geophys. Res., 102,* 24,047-24,056, 1997.

Fejer, B. G., D. T. Farley, R. F. Woodman, and C. Calderon, Dependence of equatorial *F* region vertical drifts on season and solar cycle, *J. Geophys. Res., 84,* 5792-5796, 1979.

Fejer, B. G., E. R. dePaula, I. S. Batista, E. Bonelli, and R. F. Woodman, Equatorial *F* region vertical plasma drifts during solar maximum, *J. Geophys. Res., 94,* 12,049-12,054, 1989.

Fejer, B. G., E. R. dePaula, S. A. Gonzalez, and R. F. Woodman, Average vertical and zonal *F* region plasma drifts over Jicamarca, *J. Geophys. Res., 96,* 13,901-13,906, 1991.

Fejer, B. G., E. R. dePaula, R. A. Heelis, and W. B. Hanson, Global equatorial ionospheric vertical plasma drifts measured by the AE-E satellite, *J. Geophys. Res., 100,* 5769-5776, 1995.

Fejer, B.G., E. R. dePaula, L. Scherliess, and I. S. Batista, Incoherent scatter radar, ionosonde, and satellite measurements of equatorial *F* region vertical plasma drifts in the evening sector, *Geophys. Res. Lett., 23,* 1733-1736, 1996.

Hanson, W. B., and R. A. Heelis, Techniques for measuring bulk gas motions from satellites, *Space Sci. Instrum., 1,* 493, 1975.

Hari, S. S. , and B. V. Murthy, Equatorial night-time *F*-region zonal electric fields, *Ann. Geophys., 13,* 871-878, 1995.

Maruyama, T., Modeling study of equatorial ionospheric height and spread *F* occurrence, *J. Geophys. Res., 101,* 5157-5163, 1996.

Maynard, N. C., T. L. Aggerson, F. A. Herrero, M. C. Liebracht, and J. L. Saba, Average equatorial zonal and vertical ion drifts determined from San Marco D electric field measurements, *J. Geophys. Res., 100,* 17,465-17,479, 1995.

Pingree, J. E., and B. G. Fejer, On the height variation of the equatorial *F* region vertical plasma drifts, *J. Geophys. Res., 92,* 4763-4766, 1987.

Richmond, A. D., Modeling equatorial ionospheric electric fields, *J. Atmos. Terr. Phys., 57,* 1103-1115, 1995.

Richmond, A. D. et al., An empirical model of quiet-day ionospheric electric fields at middle and low latitudes, *J. Geophys. Res., 85,* 4658-4664, 1980.

Sastri, J. H., Longitudinal dependence of equatorial *F* region vertical plasma drifts in the dusk sector, *J. Geophys. Res., 101,* 2445-2452, 1996.

Scherliess, L., Empirical studies of ionospheric electric fields, Ph.D. dissertation, Utah State Univ., Logan, 1997.

Scherliess, L., and B. G. Fejer, Storm-time dependence of equatorial dynamo zonal electric fields, *J. Geophys. Res., 102,* 24,037-24,046, 1997.

Sultan, P. J., Chemical release experiments to induce *F* region ionospheric plasma irregularities at the magnetic equator, Ph.D. dissertation, Boston Univ., Boston, Mass., 1994.

Sultan, P. J., Linear theory and modeling of the Rayleigh-Taylor instability leading to the occurrence of equatorial spread F, *J. Geophys. Res., 101,* 26,875-26,891, 1996.

Woodman, R. F., Vertical drift velocities and east-west electric fields at the magnetic equator, *J. Geophys. Res., 75,* 6249-6259, 1970.

B. G. Fejer and L. Scherliess, Center for Atmospheric and Space Sciences, Utah State University, Logan, UT 84322-4405. (bfejer@cc.usu.edu, ludger@ucar.edu)

(Received November 5, 1998; revised December 23, 1998; accepted December 23, 1998.)